A Practical Method for Assessing the Effectiveness of Vector Surge Relays for Distributed Generation Applications

Walmir Freitas, *Member, IEEE*, Zhenyu Huang, *Member, IEEE*, and Wilsun Xu, *Senior Member, IEEE*

***Abstract*—This paper presents a simple and reliable method for predicting the islanding detection performance of vector surge relays. The relay performance is characterized by a tripping-time versus power-imbalance curve. With the curve, one can determine the time taken by a vector surge relay to detect islanding for any generation-load mismatch level. The main contribution of this paper is the development of analytical formulas for directly determining the behavior of vector surge relays. As a result, efforts needed to asses the relay performance for a given distributed generation scheme can be simplified significantly. The accuracy of the formulas has been verified by extensive simulation study results.**

***Index Terms*—Distributed generation, islanding detection, synchronous generators, vector shift relays, vector surge relays.**

I. Introduction

AN IMPORTANT requirement for the connection of synchronous generators to distribution networks is the capability of islanding detection. Islanding occurs when a portion of the distribution system becomes electrically isolated from the remainder of the power system, yet continues to be energized by distributed generators. Failure to trip the distributed generators during islanding can lead to a number of problems to the generators and connected loads. Therefore, the current industry practice is to disconnect all distributed generators immediately after an islanding occurrence [1]–[5]. Typically, a distributed generator should be disconnected between 200 and 300 ms after loss of the main supply. To achieve this goal, each distributed generator should be equipped with an islanding detection device. So far, devices based on variations of frequency have been recognized as the most reliable option by the industry. Representative examples of such relays are the rate of change of frequency relay (ROCOF) and the vector surge relay (VSR), which is also known as vector shift or voltage jump relay [1]–[4].

Since the vector surge relay is one of the most sensitive frequency-based anti-islanding devices, it is selected as the study subject in this paper. Before utility engineers and distributed generator owners decide if vector surge relays are suitable for their systems, it is necessary to carry out a detailed investigation through numerous repeated dynamic simulations. The objective of this paper is to propose a systematic and practical method for directly assessing the effectiveness of vector surge relays by using simple formulas, so that time may be saved during the planning and implementation stages. In this paper, such formulas are developed and employed to determine the normalized tripping-time versus power-imbalance curves, which give a good index to evaluate the performance of vector surge relays.

This paper is organized as follows. The principle of vector surge relays is described in Section II. Section III presents the development of analytical formulas for determining the dynamic behavior of vector surge relays considering constant power loads. In Section IV, simulation results using a test system are obtained and analyzed. A modified empirical formula that extends the application to the cases of constant current, constant impedance, and aggregated loads is described in Section V. In Section VI, the modified empirical formula is evaluated by comparing the results with those obtained by detailed dynamic simulation.

Manuscript received July 7, 2003; revised September 3, 2003. This work was supported by the Alberta Energy Research Institute. Paper no. TPWRD-00358-2003.

W. Freitas and W. Xu are with the Department of Electrical and Computer Engineering, University of Alberta, Edmonton, AB T6G 2V4 Canada (e-mail: walmir@ieee.org; wxu@ee.ualberta.ca).

Z. Huang is with the Energy Science and Technology Division, Pacific Northwest National Laboratory, Richland, WA 99352 USA (e-mail: zhenyu.huang@pnl.gov).

Digital Object Identifier 10.1109/TPWRD.2004.838637

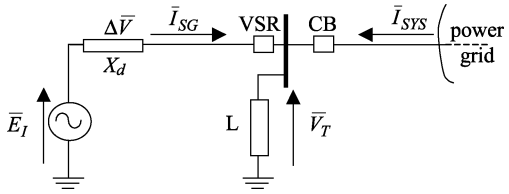

Fig. 1. Equivalent circuit of a synchronous generator in parallel with utility.

II. Principle of Vector Surge Relays

A synchronous generator equipped with a vector surge relay VSR operating in parallel with a distribution network is depicted in Fig. 1. There is a voltage drop ΔV between the terminal voltage V_T and the generator internal voltage E_I due to the generator current I_{SG} passing through the generator reactance X_d. Consequently, there is a displacement angle δ between the terminal voltage and the generator internal voltage, whose phasor diagram is presented in Fig. 2(a). In Fig. 1, if the circuit breaker (CB) opens due to a fault, for example, the system composed by the generator and the load L becomes islanded. At this instant, the synchronous machine begins to feed a larger load (or smaller) because the current I_{SYS} provided by (or injected into) the power grid is abruptly interrupted. Thus, the generator begins to decelerate (or accelerate). Consequently, the angular difference between V_T and E_I is suddenly increased (or decreased)

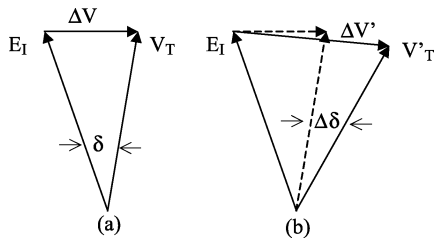

Fig. 2. Internal and terminal voltage phasors: (a) before the opening of CB; (b) after the opening of CB.

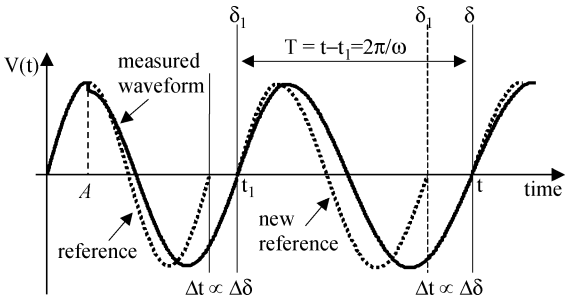

Fig. 3. Voltage vector surge and vector surge relay cycle-by-cycle measurements.

and the terminal voltage phasor changes its direction, as shown in Fig. 2(b). Analyzing such phenomenon in the time domain, the instantaneous value of the terminal voltage jumps to another value and the phase position changes, as depicted in Fig. 3, where the point A indicates the islanding instant. Additionally, the frequency of the terminal voltage also changes. This behavior of the terminal voltage is called vector surge or vector shift. Vector surge relays are based on such phenomena.

Vector surge relays available in the market measure the duration time of an electrical cycle and start a new measurement at each zero rising crossings of the terminal voltage. The current cycle duration (measured waveform) is compared with the last one (reference cycle). In an islanding situation, the cycle duration is either shorter or longer, depending on if there is excess or a deficit of power in the islanded system, as shown in Fig. 3. This variation of the cycle duration results in a proportional variation of the terminal voltage angle $\Delta\delta$, which is the input parameter of vector surge relays. If the variation of the terminal voltage angle exceeds a predetermined threshold α, a trip signal is immediately sent to the CB. Usually, vector surge relays allow this threshold to be adjusted in the range from 2 to 20°. Another important characteristic available in these relays is a block function by minimum terminal voltage. If the terminal voltage drops below an adjustable level threshold $V_{\min}$, the trip signal from the vector surge relay is blocked. This is to avoid, for example, the actuation of the vector surge relay during generator startup or short circuits.

III. Analytical Formulas for Determining the Performance of Vector Surge Relays

Considering the distributed generation system presented in Fig. 1 at steady state, the mechanical power P_M of the distributed generator is balanced with the load electrical power P_L and the electrical power P_S provided by (or injected into) the power grid. Therefore, the distributed generator rotor speed ω and angle δ are constant. After opening of the CB, the distributed generator starts running in an islanded mode and a power imbalance exists due to the lost grid power P_S. Such power imbalance ΔP, whose magnitude is equal to P_S, causes transients in the distributed generator. The dynamic behavior of the synchronous generator can be determined by using the machine swing equation. In the mathematical development below, the following assumptions are considered.

- The load is represented by a constant power model.
- The generator is represented by the classical model.
- The frequency is constant within one cycle.

The swing equation of the synchronous generator is given by

$$\begin{cases} \frac{2H}{\omega_0}\frac{d\omega}{dt} = P_M - P_L = -P_S = \Delta P \\ \frac{d\delta}{dt} = \omega - \omega_0 \end{cases} \tag{1}$$

where H is the generator inertia constant, ω_0 is the synchronous speed, and the other variables have been defined previously. The rotor angle δ can be solved from (1) as

$$\delta = \frac{\omega_0 \Delta P}{4H} t^2 + \delta_0. \tag{2}$$

Considering the cycle-by-cycle measurements shown in Fig. 3, the following angle variation can be calculated:

$$\begin{aligned} \Delta\delta &= \delta - \delta_1 \\ &= \left(\frac{\omega_0 \Delta P}{4H} t^2 + \delta_0\right) - \left(\frac{\omega_0 \Delta P}{4H} t_1^2 + \delta_0\right) \end{aligned} \tag{3}$$

$$\Delta\delta = \frac{\omega_0 \Delta P}{4H} (2t - (t - t_1))(t - t_1). \tag{4}$$

Fig. 3 shows that $(t - t_1)$ is the current cycle period, which can be approximately determined by the current frequency. Solving (1) for the angular speed, it is obtained

$$\omega = \frac{\omega_0 \Delta P}{2H} t + \omega_0. \tag{5}$$

Then, the cycle period is determined as follows:

$$T = t - t_1 = \frac{1}{f} = \frac{2\pi}{\omega} = \frac{2\pi}{\frac{\omega_0 \Delta P}{2H} t + \omega_0}. \tag{6}$$

Substituting $(t - t_1)$ in (4) by (6) and setting the rotor angle variation $\Delta\delta$ equal to the vector surge relay setting α, the following equation can be obtained:

$$\alpha = \frac{K}{2}\left(2t - \frac{2\pi}{Kt + \omega_0}\right)\frac{2\pi}{Kt + \omega_0} \tag{7}$$

where $K = \omega_0 \Delta P / 2H$. Equation (7) can be utilized to adjust the relay setting α based on the tripping time requirement and the minimum power imbalance. Rearranging such an equation generates

$$\underbrace{K^2(\alpha - 2\pi)}_{A} t^2 + \underbrace{2\omega_0 K(\alpha - \pi)}_{B} t + \underbrace{\omega_0^2 + \alpha + 2\pi^2 K}_{C} = 0. \tag{8}$$

This is a second-order equation of t, whose factors are given by the following:

- $A = K^2(\alpha - 2\pi) < 0,\ if\ \alpha < 2\pi$;
- $B = 2\omega_0 K(\alpha - \pi) < 0,\ if\ \alpha < \pi$;
- $C = \omega_0^2 + \alpha + 2\pi^2 K > 0$.

The vector surge relay setting α is usually smaller than 20°. Thus, (8) has real solutions. However, only the positive one is of interest, which is given by

$$t = \frac{-(2\omega_0 K(\alpha-\pi)) - \sqrt{\mathrm{D}_1}}{2K^2(\alpha-2\pi)} \tag{9}$$

where $\mathrm{D}_1 = (2\omega_0 K(\alpha-\pi))^2 - 4K^2(\alpha-2\pi)(\omega_0^2\alpha + 2\pi^2 K)$.

Equation (8) can also be solved to the power imbalance ΔP as follows:

$$\Delta P = \left(\frac{2H}{\omega_o}\right)\left(\frac{-2\left(\pi^2+\omega_0(\alpha-\pi)\right) - \sqrt{\mathrm{D}_2}}{2t^2(\alpha-2\pi)}\right) \tag{10}$$

where $\mathrm{D}_2 = (2(\pi^2+\omega_0(\alpha-\pi)t))^2 - 4(t^2(\alpha-2\pi)(\omega_0^2 + \alpha)$. To the usual relay setting α, note that (10) has positive real solutions.

Summarizing, the above mathematical development can be applied to the following situations.

- If the power imbalance ΔP and the tripping time requirement t are provided, one can determine the required relay setting α by using (7).
- If the power imbalance ΔP and the relay setting α are provided, one can determine the necessary tripping time t by using (9).
- If the tripping time requirement t and the relay setting α are provided, one can determine, by using (10), the minimum power imbalance ΔP which can be detected by the vector surge relay.

In this work, the validation of the mathematical development is done by using (9). This equation can be utilized to determine the performance curves of vector surge relays, as described below.

A. Performance Curves of Vector Surge Relays

The dynamic behavior of vector surge relays is strongly dependent on the active power imbalance existent in the islanded system (i.e., the mismatch between load and generation). Detecting a large mismatch is easy and quick, while a very small mismatch may not trigger the relay. Thus, an approach to evaluate the performance of these relays is to understand the relationship between tripping time and power imbalance. This relationship can be represented through a tripping-time versus power-imbalance curve as shown in Fig. 4, where each curve represents a different value of inertia constant but the same relay setting α of 10°. These curves are obtained using (9) and varying the power imbalance level of the islanded system from 1 to 0 p.u. referred to the megavolt-ampere rating of the generator. For each power imbalance level, the relay tripping time is determined since it takes time for the islanded system to exhibit detectable frequency variation.

Such curves can be employed to assess the performance of vector surge relays. For example, if it is required to trip the distributed generator within 200 ms after islanding and the inertia constant H is equal to 1.0 s, the point A can be determined. The power imbalance level in this point is the minimum power imbalance required for the vector surge relay to trip the generator within 200 ms. On the other hand, if the power imbalanced level is lower than this value, the relay will take longer than 200 ms to operate. In this paper, such a value of power imbalance is called *critical power imbalance level*.

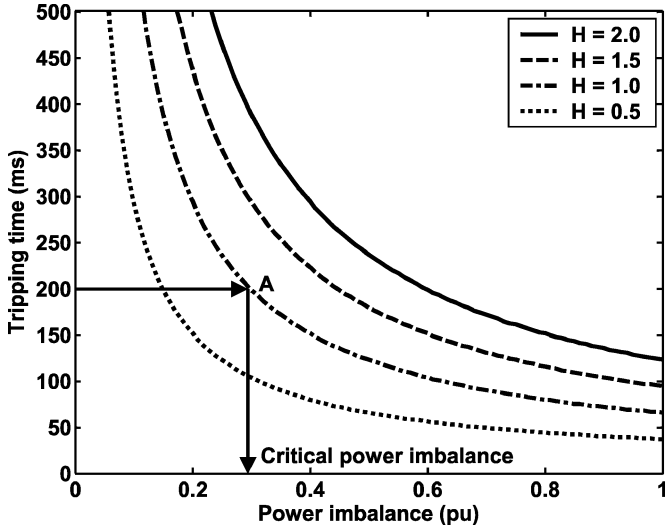

Fig. 4. Tripping-time versus power-imbalance curves for different values of generator inertia constant and constant relay setting of 10°.

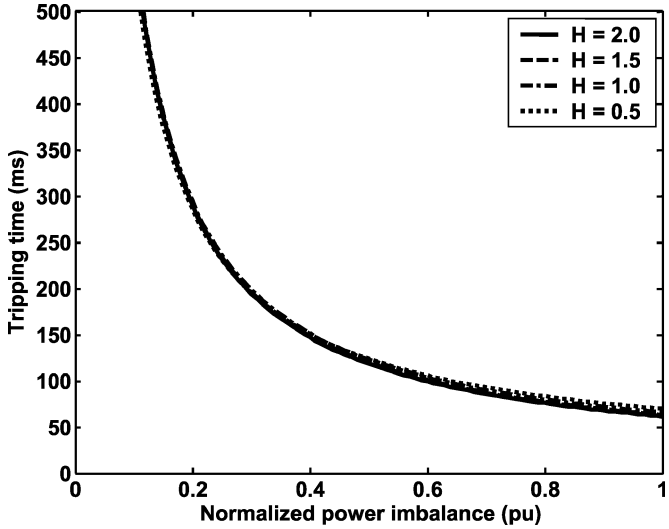

Fig. 5. Normalized tripping-time versus power-imbalance curves for different values of generator inertia constant and constant relay setting of 10°.

In Fig. 4, it can be seen that the larger the inertia constant is, the larger the critical power imbalance is for the same tripping time requirement and relay setting. A more general curve can be obtained by normalizing the values of power imbalance dividing them by the value of inertia constant, that is

$$\Delta P_{\mathrm{normalized}} = \frac{\Delta P}{H} \tag{11}$$

where $\Delta P_{\mathrm{normalized}}$ is the normalized power imbalance. In this case, there is only one normalized curve representing the performance of a vector surge relay for generators with different inertia constants. This is shown in Fig. 5.

In Fig. 6, the normalized tripping-time versus power imbalance curves are presented for different relays settings. It can be seen that the critical power imbalance is larger when the relays setting is larger. Moreover, it can be observed that when the

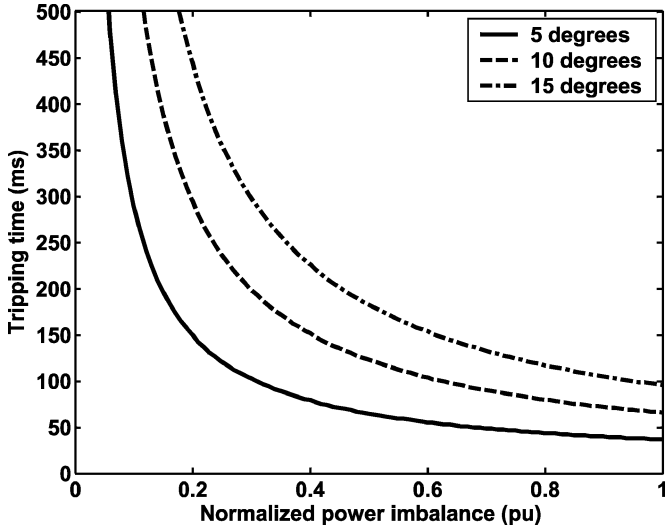

Fig. 6. Normalized tripping-time versus power-imbalance curves for different relay settings.

power imbalance decreases, the tripping time increases. This is reasonable because it takes longer for the relay to detect a small power imbalance. The increase in the tripping time is almost exponential when the power mismatch is small.

IV. Verification Studies

In this section, the accuracy of the analytical formula is analyzed. The normalized performance curves of a vector surge relay solved from the analytical formula (9) are compared with those obtained from detailed dynamic simulation. The critical power imbalances determined from both approaches are compared as well. In the case of dynamic simulation, the preislanding mismatch of active power (i.e., the system power P_S) is gradually varied from 1 to 0 p.u. by changing the generation and load profile. For each power imbalance level, dynamic simulation is conducted and the system frequency variation as a function of time is determined. The tripping time is determined once the relay activation criterion is met.

A time-domain simulation technique similar to the one utilized for transient stability studies is used for this investigation. The network components are represented by three-phase models. Distribution feeders are modeled as series RL impedances. Transformers are modeled using T circuit. The synchronous generators are represented by a sixth-order three-phase model in the dq rotor reference frame [6]. The generator is equipped with an automatic voltage regulator, which is represented by the IEEE-Type 1 model. In addition, the mechanical power is considered constant [i.e., the primer mover and governor effects are neglected, because the simulation time is short (0.5 s)].

The test system adopted in this paper is shown in Fig. 7. The network consists of a 132-kV, 60-Hz subtransmission system with a short-circuit level of 1500 MVA, represented by a Thévenin equivalent (Sub), which feeds a 33-kV distribution system through a 132/33-kV, Δ/Yg transformer. In this system, there is one synchronous generator with a capacity of 30 MVA connected at bus 5, which is connected to network through one

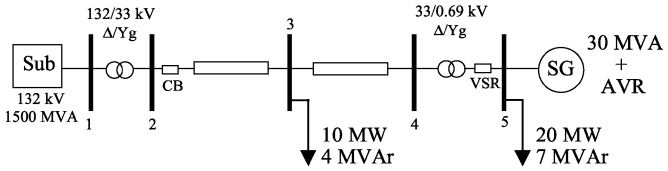

Fig. 7. Single-line diagram of the test system.

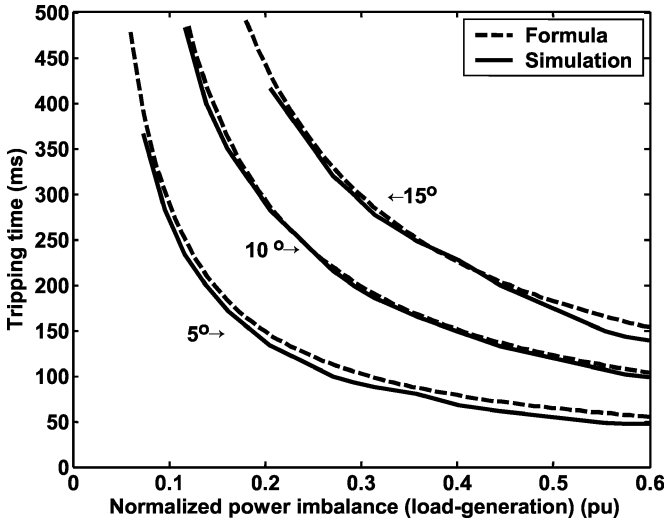

Fig. 8. Normalized tripping-time versus power-imbalance curves obtained by simulation and by the analytical formula (constant power loads).

33/0.69 kV, Δ/Yg transformer. In all simulated cases, the CB at bus 2 opens at $\mathrm{t} = 0.25$ s, which remains open during the rest of the simulation. Thus, the initial islanding power imbalance is equal to the active power provided by the substation at the islanding moment. The total simulation time is 0.75 s. Therefore, if the vector surge relay VSR installed at bus 5 does not detect the islanding condition until 0.5 s after opening of the CB, it is considered that the device is inoperative for this case. Different power imbalance scenarios are created by varying either the generator output or the total system load.

The vector surge relays are simulated as follows. The generator terminal voltage angle θ is determined at each integration step, and a reference terminal voltage angle θ_0 is computed and updated at the beginning of each cycle (i.e., it is updated cycle by cycle). The absolute variation between these two angles $\Delta\theta = \|\theta - \theta_0\|$ is calculated at each integration step and compared with the VSR angle threshold α. Additionally, the root mean square (rms) value of the terminal voltage is also determined at each integration step. If the angle variation $\Delta\theta$ is greater than the angle threshold α and the magnitude of the terminal voltage is greater than the minimum voltage setting $V_{\min}$, the vector surge relay immediately sends a trip signal to the CB.

In Fig. 8, the normalized performance curves obtained by simulation and by the analytical formula are presented considering three different relay settings α. It should be pointed out that the loads are represented by constant power models for all of the curves. Very good match can be observed between the two sets of the relay performance curves.

The values of critical power imbalance determined by the analytical formula and simulation are shown in Table I. In this

TABLE I
CRITICAL POWER IMBALANCE OBTAINED BY THE ANALYTICAL FORMULA AND DYNAMIC SIMULATION

α (degrees)	Tripping time (ms)	Critical power imbalance (%)		Power difference (%)
		Simulation	Formula	
2	200	8.4	8.8	-0.4
	300	5.5	5.8	-0.3
5	200	20.8	22.0	-1.2
	300	23.6	24.5	-0.9
10	200	43.7	44.7	-1.0
	300	29.0	29.4	-0.4
15	200	66.5	68.0	-1.5
	300	43.7	44.7	-1.0
20	200	86.2	92.1	-5.9
	300	56.9	60.5	-3.6

table, the usual values of relay settings α and tripping time requirements are presented. The fifth column in this table gives the difference between the simulation results and the formula. It can be observed that the differences are very small, and the formula exhibits satisfactory accuracy. It is worth noting that the results obtained by the formula are slightly conservative (i.e., the critical power imbalances are slightly larger).

Good accuracy of the analytical formula considering constant power loads has been further confirmed utilizing other distribution systems. However, such accuracy is not expected for the case of constant current and constant impedance loads due to the limitation caused by the assumption of constant power models. To extend the application of this formula to other load models, further investigation is needed. The following section focuses on the characteristics of constant current and impedance loads. An empirical power imbalance factor is proposed to modify the analytical formula, allowing constant current, constant impedance, and aggregate loads to be accurately analyzed.

V. MODIFIED EMPIRICAL FORMULA FOR GENERAL CASES

The analytical formula developed in the previous sections considers that the power imbalance after opening of the CB is constant. However, it occurs only if the loads have characteristics of constant power. In the case of voltage-dependent loads, the power imbalance after islanding has a dynamic behavior and it can either increase or decrease. Thus, it is necessary to consider this variation. However, it is very difficult to analytically determine how much the power imbalance changes. It depends on the characteristics of the distribution network and generator as well as the operating point. Thus, in the following sections, an empirical formula to estimate the power imbalance is proposed based on the observation of numerous cases simulated considering different load characteristics.

Typical loads can be represented by the combination of constant impedance, constant current, or constant power models. Simulations are carried out to study the three different load models using the test system in Fig. 7. The dynamic behavior of these different loads during islanding is presented in Fig. 9. In this case, the synchronous generator is injecting 20 MW into the network at the islanding instant (0.25 s). It can be observed that the active power consumed by constant current and constant impedance loads decreases after islanding. This fact occurs due to the reduction of the voltage profile at load buses. It is important to mention that the reduction of the voltage profile always occurs in an islanded system. This has been verified in various systems operating at different points. The difference is how intense this voltage depression is. Therefore, an empirical factor should be introduced to correct the values of power imbalance ΔP in the analytical formula (9). Here, this factor is called *power imbalance factor*.

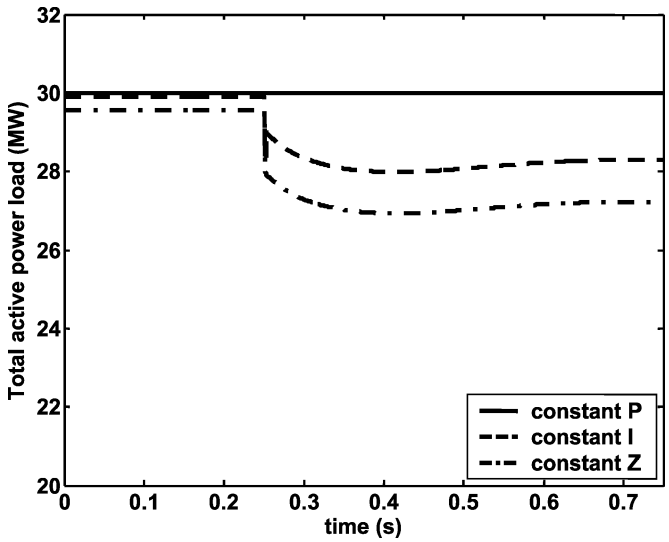

Fig. 9. Dynamic behavior of the total active power load during islanding considering different kinds of loads (synchronous generator injecting 20 MW).

A. Power Imbalance Factor

Active power loads can be represented by an exponential voltage-dependent model as follows [6]:

$$P = P_o \left(\frac{V}{V_o} \right)^{np} \tag{12}$$

where P is the active power, V is the nodal voltage, the subscript "$_0$" indicates nominal values, and np represents the relationship between active power and nodal voltage of the load. Usually, np is in the range from 0 to 2 [6]. np equal to 0, 1, and 2 represents constant power, constant current, and constant impedance loads, respectively. An index NP_T can be defined as below to represent the aggregate load characteristics of the total active power load of the system

$$NP_T = \sum_{i=1}^{nbus} \frac{P_i}{P_T} np_i \tag{13}$$

where P_T is the total active power load of the system, $nbus$ is the total number of buses in the system, and P_i is the active power load at bus i. NP_T also falls into the range from 0 to 2. The power imbalance factor should reflect the behavior of the system load as verified in Fig. 9. Thus, if the system loads are constant power, the power imbalance should be considered constant after the opening of the CB. On the other hand, if the system loads present constant current or constant impedance characteristics, the power imbalance should change consider-

ably after the opening of the CB due to the power demand decrease. The larger NP, the larger power imbalance variation. However, it is very difficult to analytically determine how much the power imbalance would change after islanding.

Based on extensive simulations carried out in different systems with different distributed generators, it has been observed that the largest variation of power imbalance always occurs in the case of constant impedance loads. Furthermore, this variation usually varies from 10–30%, it depends on the characteristic of the system and generator as well as the operating point. Thus, roughly considering the average power imbalance variation after the opening of the CB for constant impedance loads equal to 20%, the following power imbalance factor ($P_{\rm fac}$) can be obtained by using linear interpolation:

$$0 < NP_T < 2 \quad \text{and} \quad 1.2 \geq P_{\rm fac} \geq 0.80 \tag{14}$$

$$P_{\rm fac} = 1 \pm \frac{NP_T 0.2}{2}. \tag{15}$$

The "±" sign is determined by the sign of the power imbalance after opening of the CB. If there is a deficit of electric power, the adopted sign is negative, while excessive electric power takes the positive sign. In the case of power deficit (or excess), the power imbalance increases (or decreases) after the opening of the circuit breaker due to load reduction. Moreover, the larger NP_T, the larger the variation in the values of power imbalance. On the other hand, if NP_T is zero (constant power loads), the power imbalance should be kept constant. Furthermore, based on the results presented in the previous sections, it can be verified that the tripping time increases almost exponentially when the power imbalance decreases. Thus, the power imbalance factor given by (15) should not be applied directly to different values of power imbalance. Adopting that the power imbalance factor affects the power imbalance in an exponential way, the final power imbalance ΔP_F can be calculated as (16) and then this power imbalance replaces ΔP in (9) to determine the VSR performance

$$\Delta P_F = \Delta P_o^{\left(\frac{1}{P_{\rm fac}}\right)} \tag{16}$$

where ΔP_0 is the initial power imbalance value at the instant of the opening of the CB. It is important to note that the power imbalance is not affected in the case of constant power loads ($NP_T = 0$ and $P_{\rm fac} = 1$).

VI. Verification Studies of the Modified Formula

This section employs dynamic simulation to examine the accuracy of the modified empirical formula. The test system and modeling are the same as those described in Section IV. Figs. 10 and 11 show the normalized tripping-time versus power-imbalance curves, for constant current and impedance loads, respectively, obtained by simulation, the analytical formula, and the modified empirical formula. In these figures, the relay setting α is of 10°. In both figures, two distinct situations are analyzed. One corresponds to the case of power deficit in the islanded system and the other one corresponds to the case of power excess. For the power deficit cases, the simulation results are obtained by keeping the system total load constant but varying the active power injected by the generator into the network from 1 to 30 MW. While for power excess cases, simulations are conducted by keeping the generator output constant at 30 MW but varying the total active power load from 30 to approximately 0 MW, maintaining the original power factor.

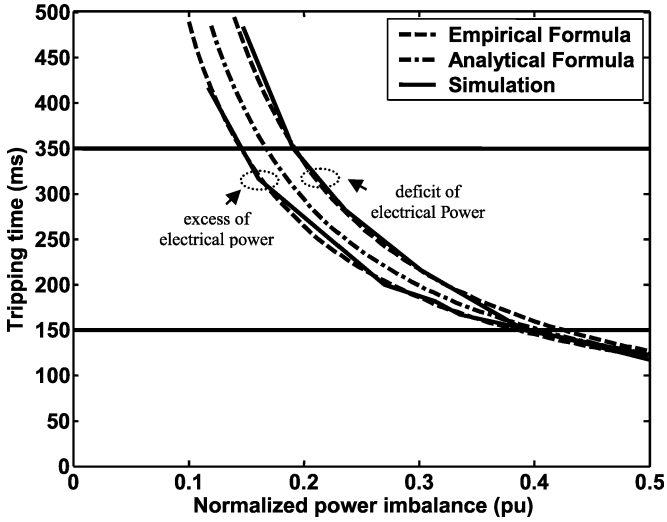

Fig. 10. Normalized tripping-time versus power-imbalance curves obtained by simulation and by the modified empirical formula (constant current loads).

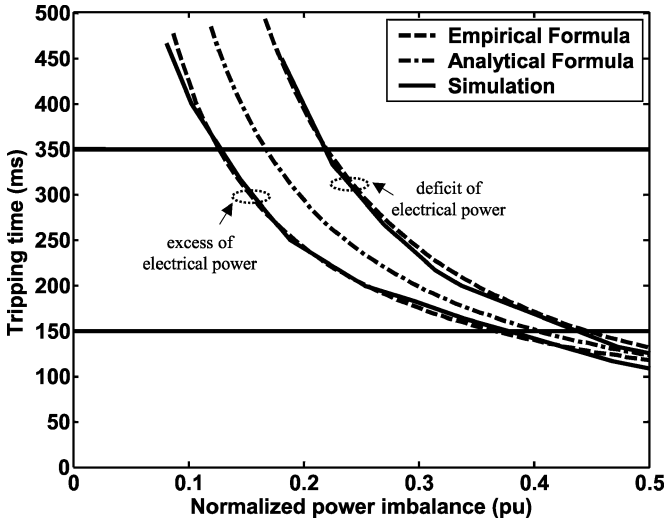

Fig. 11. Normalized tripping-time versus power-imbalance curves obtained by simulation and by the modified empirical formula (constant impedance loads).

The results for constant current loads in Fig. 10 show that the curve provided by the analytical formula is in the middle between the situation with deficit and excess power. The modified empirical formula presents a good performance of matching the simulation curves, especially for the range of tripping time from 150 to 350 ms.

The constant impedance load case is shown in Fig. 11. Again, the modified empirical formula presents a good performance in the range of interest. Furthermore, based on the results shown in Figs. 10 and 11, it can be observed that the most conservative case (i.e., the case with the largest value of critical power imbalance to a determined tripping time requirement) occurs when the loads have characteristics of constant impedance in a system

TABLE II
CRITICAL POWER IMBALANCE OBTAINED BY THE EMPIRICAL FORMULA AND DYNAMIC SIMULATION: THE MOST CONSERVATIVE CASE

α (degrees)	Tripping time (ms)	Critical power imbalance (%)		Power difference (%)
		Simulation	Modified Formula	
2	200	18.0	14.3	3.7
	300	15.1	10.2	4.9
5	200	30.4	29.8	0.6
	300	23.3	21.3	2.0
10	200	50.5	52.5	-2.0
	300	37.1	37.5	-0.4
15	200	70.8	73.5	-2.7
	300	50.5	52.5	-2.0
20	200	91.7	93.6	-1.9
	300	64.8	66.9	-2.1

with deficit of power. For this most conservative case, the critical power imbalance obtained by simulation and by the empirical formula is compared in Table II. From the fifth column, showing the gap between simulation and the formula, it can be noted that the modified empirical formula is able to predict the effectiveness of vector surge relays with reasonable accuracy. It is worth mentioning that other systems have been analyzed, and similar performance with the empirical formula has been observed.

In summary, the simulation results validate the method proposed in this paper for the performance evaluation of vector surge relays. The analytical formula derived in Section III defines the performance curve of a vector surge relay and lays a solid foundation for the work in this paper. The concept of critical power imbalance is developed to quantify the evaluation process. While the analytical formula itself can be well applied to the cases of constant power loads, the application is extended to the cases of more typical voltage-dependent loads by modifying the power imbalance [i.e., by substituting ΔP in (9) by (16)]. The general form of the formula becomes

$$t = \frac{-(2\omega_0 K(\alpha-\pi)) - \sqrt{\mathrm{D}_1}}{2K^2(\alpha-2\pi)} \tag{17}$$

where $D_1 = (2\omega_0 K(\alpha-\pi))^2 - 4K^2(\alpha-2\pi)(\omega_0^2\alpha + 2\pi^2 K)$ and $K = \omega_0(\Delta P_0)^{(1/P\mathrm{fac})}/2H$.

Accordingly, formulas similar to (7) and (10) can be developed for other applications as was discussed in Section III.

VII. CONCLUSION

This paper has presented a new method for directly assessing the effectiveness of vector surge relays based on a systematic and practical formula. A good foundation for the developed formula is established by rigorous analytical derivation with constant load assumption. To cope with practical cases where loads usually exhibit an aggregate voltage-dependent characteristic, an empirical factor is proposed to incorporate power imbalance variations into the analytical formula. An extensive comparison between the formula calculation and simulation results shows that the proposed formula can predict the performance of vector surge relays with good accuracy.

The proposed method can be utilized to avoid time-consuming simulations at the planning and implementation stages of vector surge relays. Although the results presented in this paper are based on only one test system, studies have also been conducted in other systems. The conclusions are quite similar. Note that in a real system, the total tripping time should include the actuation time of the CB employed (usually between two to five cycles). This will shift the tripping-time versus power-imbalance curves upward and result in larger critical power imbalances. However, the method presented in this paper is still applicable.

ACKNOWLEDGMENT

The authors thank the utility companies in Alberta (ATCO, EPCOR, ENMAX, and AQUILA) for their expert advice on this project.

REFERENCES

[1] *IEEE Guide for Interfacing Dispersed Storage and Generation Facilities With Electric Utility Systems*, 1988.
[2] *G59/1 Recommendations for the Connection of Embedded Generating Plant to the Regional Electricity Companies Distribution Systems*, 1991.
[3] Working Group 37.23, "Impact of Increasing Contribution of Dispersed Generation on the Power System," CIGRÉ, Tech. Rep., Paris, France, 1999.
[4] CIRED Working Group 4, "Dispersed Generation," CIRED, Tech. Rep., Liege, Belgium, 1999.
[5] N. Jenkins, R. Allan, P. Crossley, D. Kirschen, and G. Strbac, *Embedded Generation*, 1st ed. London, U.K.: Inst. Elect. Eng., 2000.
[6] P. Kundur, *Power System Stability and Control*. New York: McGraw-Hill, 1994.

Walmir Freitas (M'02) received the B.Sc and M.Sc degrees in electrical engineering from the Universidade Estadual Paulista (UNESP), Sao Paulo, Brazil, in 1994 and 1996, respectively, and the Ph.D degree in electrical engineering from the Universidade Estadual de Campinas (UNICAMP), Sao Paulo, in 2001.

Currently, he is a Postdoctoral Fellow with the University of Alberta, Edmonton, AB, Canada. His research interests include power system stability and control, distributed generation, and power-electronic applications.

Zhenyu Huang (M'01) received the B.Eng. degree from Huazhong University of Science and Technology, Wuhan, China, in 1994 and the Ph.D. degree from Tsinghua University, Beijing, China, in 1999.

Currently, he is a Development Engineer with the Energy Science and Technology Division, Pacific Northwest National Laboratory, Richland, WA. From 1998 to 2002, he conducted research at McGill University, Montreal, QC, Canada; the University of Alberta, Edmonton, AB, Canada; and the University of Hong Kong. His research interests include power electronics, power system stability, and power quality.

Wilsun Xu (SM'93) received the Ph.D. degree from the University of British Columbia, Vancouver, BC, Canada, in 1989.

Currently, he is a Full Professor of electrical engineering at the University of Alberta, Edmonton, AB, Canada, where he has been since 1996. From 1989 to 1996, he was an Electrical Engineer with BC Hydro, BC, Canada. His research interests are power quality and power system stability, and he has recently started to research distributed generation-related subjects.